UDC 621
DOI: 10.15587/1729-4061.2022.266256

DESIGN AND PERFORMANCE STUDY OF A DUAL-AXIS SOLAR TRACKER SYSTEM FOR THE CLIMATE OF EASTERN LIBYA

Ali Najim Abdullah Saieed
Assistant Lecturer, Master Degree
Department of Air-Conditioning and Refrigeration Engineering Technology
Al-Rafidain University College-Baghdad
Hay Al-Mustansiriya, Mahala, 506, Baghdad, Iraq, 10001
Monaem Elmnifi
Master of Energy Technologies, Lecturer
Department of Mechanical Engineering
Bright Star University
Tourist Road str., 31, Brega, Libya
Abdalla Saad Ahmed Eltawati
Engineer
Waha Oil Company
Dubai str., 14, Benghazi, Libya, 16063
Salem E Salem Elzwa
Master of Science System and Control, Assistant Lecture
Ajdabiya College
Higher Institute of Comprehensive Professions Ajdabiya
Istanbul str., 22, Ajdabiya, Libya, 2531
Yasir Ali Mezaal
Lecturer Doctor
Department of Finance and Banking
College of Administration and Economics
Al-Farahidi University
Baghdad, Iraq
Laith Jaafer Habeeb
Corresponding author
Assistant Professor Doctor
Training and Workshop Center
University of Technology
Al-Sina'a str., 62, Al-Wehda neighborhood, Baghdad, Iraq, 10001
E-mail: 20021@uotechnology.edu.iq

Fossil fuels are non-renewable, finite, and exhausting. Therefore, it is necessary to find alternative sources of energy. Solar energy is abundant in nature, so it can be considered as the best alternative to meet the energy demand. It is sustainable, renewable, and scalable. Increasing the efficiency of harnessing solar energy should be one of our top concerns because it is a renewable resource. The challenge in utilizing this energy is to increase efficiency as well as reduce production costs. So, a dual-axis solar tracker was developed in this study to ensure that the tracked solar cells create more electrical energy than stationary solar cells, improving the performance of the solar panels and expanding their ability to make the most of the solar radiation. The experiment yielded great results. Due to its constant exposure to sunlight, the temperature of the mobile cell is higher than that of the stationary cell. The radiation intensity of the tracked cell is more than that of the fixed cell. The radiation intensity for the traced cell is more than that of the fixed cell and peaks at 1282 W/m^2 on September 10 and 1028 W/m^3 on September 11. For day 10, there was a daily rate of rise in radiation intensity on the tracker cell of 42 % compared to the fixed. Day 11 saw a difference of 210 $W/m^2/h$, or 61 percent. The results are almost same from midday until dusk. During the day, the tension in the vacuum is somewhat different for stationary cells and tracking cells, with the value of the tracker being marginally lower than the fixed value. The increased temperature in the cell caused by more solar radiation and a warmer environment is thought to be the reason for the lower energy gain in the tracker

Keywords: solar tracker, light dependent resistor (LDR), Arduino, solar cells, dual-axis

Received date 07.08.2022
Accepted date 21.10.2022
Published date 30.10.2022

How to Cite: *Najim Abdullah Saieed, A., Elmnifi, M., Saad Ahmed Eltawati, A., E Salem Elzwa, S., Mezaal, Y. A., Jaafer Habeeb, L. (2022). Design and performance study of a dual-axis solar tracker system for the climate of Eastern Libya. Eastern-European Journal of Enterprise Technologies, 5 (8 (119)), 79–88. doi: https://doi.org/10.15587/1729-4061.2022.266256*

1. Introduction

To resolve fossil fuels' role in the world's energy issue, the sun's energy can be used as a clean, alternative energy source because it is always there. Solar radiation is largely responsible for both the renewable and non-renewable energy sources that are available on Earth's surface. Along with secondary energy sources such as wind and biomass energy, all of them, including coal, oil, and gas, were created over time as a result of sunlight and the subsequent heat and pressure [1]. Global warming is a result of the depletion of fossil fuel resources and the rise in harmful gas emissions, which caused climate change. Finding answers and substitutes that will guarantee a constant supply of the energy you require on the one hand

while maintaining the environment's safety on the other, has become important. The photoelectric conversion mechanism is another way that solar energy can be turned into electricity. This is done by using photovoltaic solar cells to directly convert solar or photovoltaic radiation into electricity [2]. The field of converting solar energy to electricity, or photovoltaics, has received the lion's share of research funding and application development. Since energy is produced and used in the same location, the generation is centralized, which reduces the need for extensive transportation. There is still a lack of demand for solar power plants [3].

Therefore, studies that are devoted on the design and performance of a dual-axis solar tracker system for the climate of eastern Libya are scientific relevance.

2. Literature review and problem statement

Numerous studies have been conducted to enhance and boost the generation of electrical energy via solar energy conversion. A biaxial solar tracker among these tests that could endure severe weather and track elevation and azimuth movement was proposed [4]. A solar panel, frame, base, pivot frame, and first and second motors are all components of the solar tracker. On the frame, solar panels were put to collect light. The solar panel's height movement is controlled by the first motor, while its azimuth movement is controlled by the second motor. The work was done in different conditions and days than our current research. The possible system benefits for straightforward solar system tracking employing a stepper motor and light sensor were indicated by [5]. According to reports, the solar tracking device was created and tested on an experimental basis. Details of the design and the experimental findings were addressed. Small solar cells were used in the design of the solar tracker to serve as self-adjusting sensor systems, giving the device a variable indication of its angle in relation to the sun via measuring voltage output. The solar tracker was found to be effective in maintaining the solar panels at a vertical angle to the sun using this technique. Here a review was done rather than an experimental work. A fixed horizontal arrangement resulted in a 30 % improvement in strength. According to [6], studies have shown that a solar tracking system with uniaxial freedom can boost energy output by about 21 %, while a dual axis dual-axis tracking system can boost output by more than 41 %. As a result, the goal of this effort was to create and put into use a solar tracking system with complete degrees of freedom. The brain of the entire tracking system, this controller terminal was programmed to detect sunlight via the sensors and then move the motor to a position where the solar panel's surface could get the most light. This was programmed to put the solar panels where they could receive the most sunshine by positioning photovoltaic cells to detect sunlight. Different equipment was used as well as different boundary conditions and place in comparison to our study. One of the reasons for the solar tracker, according to [7], was that solar radiation was continuously striking perpendicular to the flat plate collector. This resulted in the production of 1.4 times as much heat energy as a stationary collector of the same size. A complex rig was used to do the practical work with different parameters when compare it with present work. A cost-effective intelligent solar tracking system was designed and tested by [8] to capture the maximum amount of solar energy. The PIC 18F452 was small and designed to be operated by a controller. Two mechanisms formed the system's foundation. The PILOT search engine, which finds the sun's location, was first. Smart panels, the second mechanism, were only aligned with PILOT if the maximum amount of energy could be harvested. Description of a biaxial solar tracker capable of withstanding extreme weather conditions and following elevation and azimuth motion. The solar tracker includes a solar panel, frame, base, pivot frame and first and second motors. This is a review paper not an experimental work. Solar panels were installed on the frame and capture sunlight [9]. The solar tracker is intended to use tiny solar cells to function as self-adjusting sensor systems, delivering a changeable indication of the tracker's relative angle to the sun by sensing the output of a voltage detector. A new control strategy for tracking was used and it was not an easy system. In 2017, comparison to the stationary system, the gain increase owing to active tracking is roughly 30 %, according to the study [10]. The water temperature of the solar tracker's still photos was found to be higher than that of the terrestrial vehicle. Also, it is a review article rather than a practical work. In the winter, tracking can boost water production by up to 31 % in solar water purifiers for drinking water from the sun during the winter months [11]. Here a tracking system was used to produce water not an electricity. A dual axis solar tracking system was created, put into use, and reviewed by another researcher employing light-dependent resistor sensors, direct current motors, and a microprocessor to enable uninterruptible power supply for rural applications [12]. The experiment's findings demonstrated that the suggested system was more economically viable and generates 31.4 % more energy than a single axis tracking system and 67.9 % more than a fixed PV panel system. Different rig, boundary conditions and site were used to check the tracking system. To ensure maximum energy gain, [13] also provided the design and installation of the Dual Axis Solar Tracking System. The device automatically alters its orientation to obtain the highest light intensity as the light intensity drops. A small solar system for lighting was used in this study.

The majority of the researches related to this work are in the design of a single or dual-axis solar tracker, thus we focused on the design of a two-axis tracker in this work to understand the changes that occur to the solar cell in atmospheric conditions of eastern Libya. In the previous studies, the references that approved were supposed to list some ideas that were similar to the subject of the study in terms of design, installation, and testing of the tracker. Therefore, what is new and developed in this study is that the two-axis solar tracker was designed and applied according to the weather conditions of the study area, Libya, for the first time due to the high temperature in this region. Therefore, there was a rise in the temperature of the moving cell.

3. The aim and objectives of the study

The aim of this study is to design of a two-axis tracker to understand the changes that occur to the solar cell in atmospheric conditions. This will make it possible to improve the efficiency of the solar panels and increased their capacity to utilize solar radiation.

To achieve this aim, the following objectives are accomplished:

– to compare the temperature of the solar cell;

– to compare the intensity of solar radiation falling on the solar cell;

– to show the short circuit current (isc);
– to find the open circuit voltage (voc);
– to present the power output versus time as a tracker and fixed.

4. Materials and methods

4. 1. Object and research hypothesis

In order to reach this goal and due to the lack of a ready-made solar tracker, we had to start work to design and implement a dual-axis horizontal solar tracker to track the solar azimuth and a vertical one to track the sun's elevation angle during daylight hours. It has been used to improve the performance of the photovoltaic solar cell.

The idea is to rotate the axis about the vertex with the angle of rotation to the azimuthal angle (γ). While the other axis is parallel to the Earth's surface and rotates at an angle of rotation equal to the angle of elevation (α). Trackers (elevation/azimuth) are devices that employ astronomical data or algorithms for the sun to calculate the position of the sun at any given time and location on the earth's surface. The location, date and time of the tracker is entered by the microcontroller to fix the position of the sun, or it needs a sensor for sunlight to control the motors that direct the panels towards the sun as shown in Fig. 1 [14].

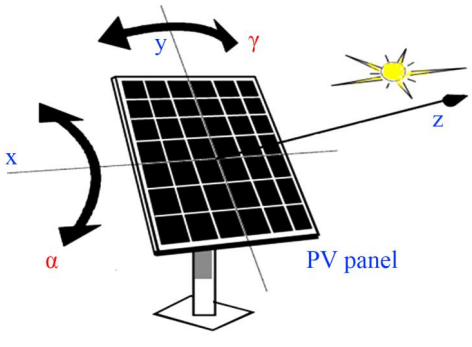

Fig. 1. Dual axis solar tracker model

This type of Dual axis solar tracker was designed in this research using a solar cell, an Arduino panel, a charging battery, mechanical motors and an LED lamp.

Analyzing the results, what was achieved in this study and what we needed and focused on were explained and analyzed. For example, the produced current, the voltage and the efficiency of each cell, and the change in temperature were explained and analyzed.

4. 2. Study site

This inquiry focused on Al-Marj Libya as a case study, and the meteorological and energy data needed for the experiment's conception and implementation. It is calculated that the average yearly solar radiation is 2.900 kWh/m^2, with more than 3.300 hours of sunshine [15].

The Al-Marj sun chart shows how the sun moves throughout the year and at different times of the day. The fixed collectors are installed in a location where the gross solar energy obtained is higher than most of the predetermined locations. This results in a significant reduction in expenses and the preservation of collectors as Fig. 2, 3.

The chart can be used to determine the position of the sun at various times and seasons so that the panel can be adjusted for maximum output. In tropical areas like Libya, fixed trackers are less expensive. For countries located beyond plus +10 degrees north and minus –10 degrees south of the equator, serious tracking is required. This is due to the fact that the location of the midday sun varies greatly. The sun is at its highest between 12^h and 14^h, according to the chart. Because the collectors are obliquely angled to the sun outside of this range, only a percentage of the light reaches the absorption surface.

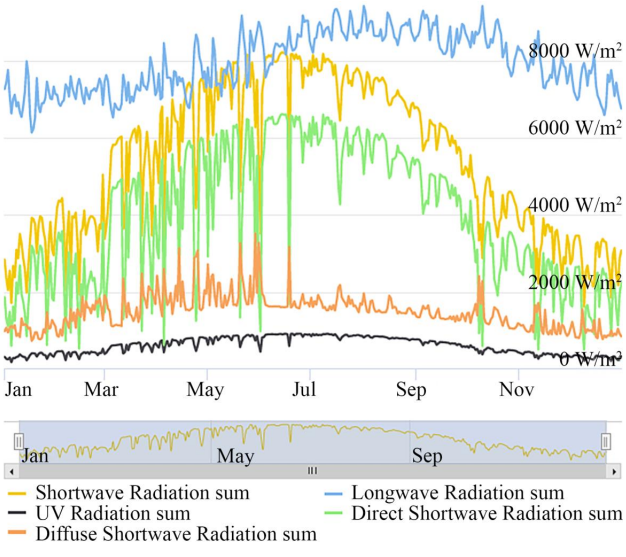

Fig. 2. Components of solar radiation for the study site for the year 2021

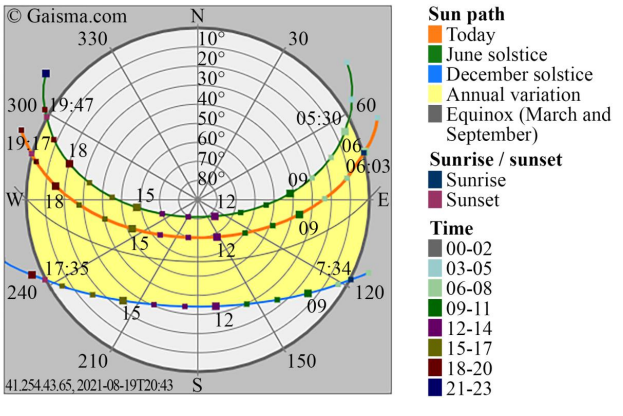

Fig. 3. Al-Marj sun path diagram

4. 3. The suggested solar tracking system's design

The suggested solar tracking system must meet the following technical requirements related to the investigated application:

1) lowest energy consumption, in order to maximize the installation's overall efficiency and achieve the best performance-cost ratio;

2) operational reliability, under a variety of disturbance situations;

3) the capacity to connect the system into a centralized monitoring and control structure, resulting in a digital control solution; the ability to lower the cost of the mobility solution while increasing its viability; (motor, gears, sensors);

4) a centralized framework for monitoring and control with the capability of system integration results in a digital control solution.

The following components are included in the suggested model for driving photovoltaic panels:

1) with current monitoring but no movement sensors, a voltage-mode DC (Direct Current) electric motor with current monitoring and no movement sensors is driven;

2) a motor control system of the intelligent drive type that is entirely digital, which allows for the digital control of the motor as well as the implementation of the PV panel orientation application in a motion control language that has been developed specifically for this application;

3) a light intensity measuring device that is attached to the PV panel and serves as the sensor that directs the movement of the solar panel.

4. 4. Optical sensors

The photoresistor LDR, whose light-dependent resistance is a variable resistance, is one of the optical sensors that are often employed. In Fig. 4, the resistance of the LDR is demonstrated to be inversely proportional to the intensity of the light, with a maximum resistance in the absence of light and a lowest resistance in the presence of light, as indicated in the graph. In addition to being inexpensive in cost and simple to connect, an LDR has a reasonable reaction time when exposed to light, it is bidirectional and has a long-life expectancy when used in an environmental setting. In order to build a dual axis solar tracker, it is necessary four photoresistors, the performance of which is mostly determined by comparing the values that the resistors provide, Fig. 5.

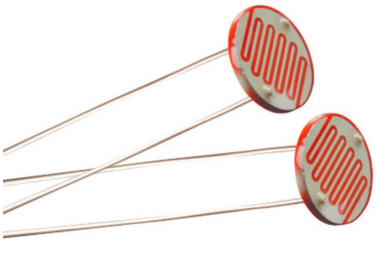

Fig. 4. Optical sensors light-dependent resistance

Fig. 5. Optical sensor installation model

The main objective through the use of a solar tracking system is to constantly maintain the photovoltaic panels facing the sun. This will increase the amount of radiation received and thus increase the electrical energy produced. To achieve this, our sensor must have a very precise architecture, and its design is as shown in Fig. 5.

4. 5. Arduino

Arduino is an open-source platform that allows to create electronic creations with minimal effort, Fig. 6, 7. A microcontroller and a programming portion are both included in the Arduino board. The programming part is an integrated development environment that runs on a computer and is used to write and upload code to the Arduino board from the computer.

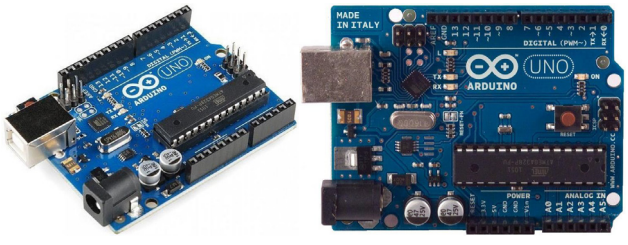

Fig. 6. Arduino board

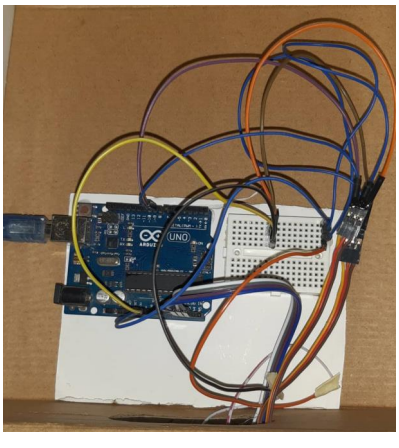

Fig. 7. Tracker Control Circuit

To connect the model, the sensors were collected in a board, to control the four directions that the sun tracking system can take: east, west, north and south, and it is connected on one side to the Arduino board, and on the other hand to one of the motors that control the movements of the two axes as shown in Fig. 7.

4. 6. Mechanical part

The mechanical part is also important in the embodiment of the solar tracker and is responsible for raising the solar panels and moving them in the four directions (North. South. East and West) as shown in Fig. 8.

Fig. 8. Direct Current motor

In the solar tracking system, the mechanical movements are ensured by the direct current actuators, Fig. 8, in order to facilitate their direct operation thanks to the photovoltaic panels.

4. 7. Structure design

SolidWorks software (Waltham, Massachusetts, United States) was used to design the solar tracker, Fig. 9.

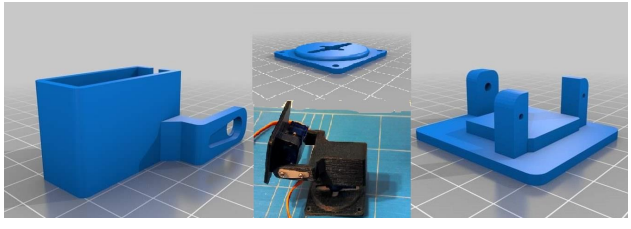

Fig. 9. The structure of the solar tracker

It can be applied in the real world. The main parts designed for the system are shown in Fig. 9.

4. 8. Analysis of the results of the experiment

In this part, let's compare the intensity of solar radiation on a fixed solar cell, with a two-axis solar tracker, on September 10 and 11, 2021. The model was installed on the roof of a house in Al-Marj city to conduct the experiment. Where two photovoltaic solar cells were installed, one on the structure of the solar tracker and the other fixed oriented towards the south at an angle mil 32, with a power of 1.4 watts and a voltage of 0.5 volts. Fig. 10 and Table 1 show the specifications of the solar panel and the type of cell used.

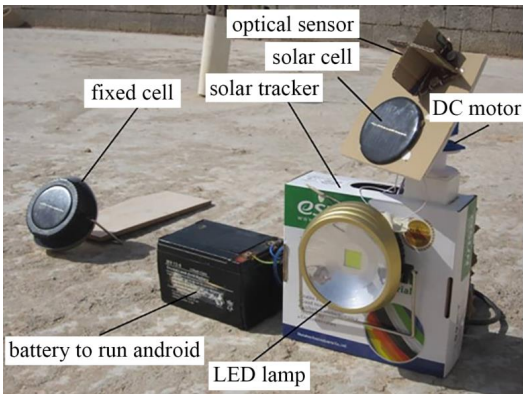

Fig. 10. Solar cell with solar tracker and fix

Table 1

Specifications of the solar panel and the type of cell used

Module Type	50M (36) Divel Solaire
Maximum Power	50 W
Voltage at pmax (Vmp)	18 V
Open circuit voltage (Voc)	21.87 V
Cells 36 cs, 156×63 monocrystalline silicon	–
Weight	6 kg
Short circuit current (Isc)	3 A

The measurements were made every hour throughout the day (from sunrise to sunset), as the solar tracker rotates at azimuth and elevation angles during the study period.

4. 9. Solar Constant

Here, it is about the flux of solar radiation on a typical surface of sunlight outside the Earth's atmosphere at me, at a distance between the Earth and the Sun of e. The solar constant is presently accepted to be 1370 W/m^2, which is the current accepted value. A small elliptical orbit of the Earth causes the extraterrestrial radiative flux to vary from a high of 1.418 W on January 3 to a low of 1.325 W/m^2 on July 4, depending on the time of year [16].

A structure's total solar radiation gain may be calculated by first figuring out how much solar radiation is reflected off of the structure's various surfaces. Solar radiation reaching a surface per unit area is quantified in watts as total surface solar radiation. This information is provided by:

$$I_{i\theta} = I_{DN}\cos\theta + I_{d\theta} + I_{r\theta}, \quad (1)$$

where $I_{i\theta}$ – total solar radiation of a surface, W/m^2; I_{DN} – direct radiation from the sun, W/m^2; $I_{d\theta}$ – radiation diffuse from the sky, W/m^2; $I_{r\theta}$ – short-wave radiation reflected from other surfaces, W/m^2; θ – angle of occurrence, degrees.

Direct radiation from the sun (IDN): Many solar radiation models are available for estimating the sun's direct radiation. One of the co computations proposed by ASHRAE is the one below. The direct radiation lo, according to this model, is provided by:

$$I_{DN} = A.\exp\left[-B/\sin B\right]. \quad (2)$$

For the months of December and January, the apparent solar irradiation (A) is considered to be 1230 W/m^2, while for the middle of summer, it is taken to be 1080 W/m^2. The constant Bis, also known as the atmospheric extinction coefficient, has a value of 0.14 in the winter and 0.21 in the summer, depending on the season. In either form, either equations of tables or empirical data are given for the values of A and B for each 21″ day of each month that has been calculated [17].

Diffuse radiation $I_{d\theta}$ from a clear sky, according to the ASHRAE model, is provided by the following equation:

$$I_{d\theta} = C \cdot I_{DN} \cdot F_{ws}. \quad (3)$$

The value of C is considered to be constant for a clear sky on an average day of the month under cloudless conditions. A table with the average monthly data has been created and is accessible for viewing and downloading. For mid-summer, the value of C may be considered as 0.135, while for winter, it can be taken as 0.058. The view factor or configuration factor, also known as the F_{WS} factor, is the fraction of diffuse radiation incident on the surface that is used in the calculation. The F_{WS} of diffuse radiation is only a function of the direction of the surface in the case of diffuse radiation. It is straightforward to demonstrate that this is equal to:

$$F_{ws} = \left(1+\cos\varepsilon\right)/2, \quad (4)$$

where ε is the tilt angle in degrees. Clearly, for horizontal surfaces (ε=0°), the factor F_{ws} is equal to 1, but for vertical surfaces (ε=90°), the factor F_{ws} is equal to 0.5. This mode holds strictly true in the case of a cloudless sky, where radiation from the sky falls evenly on the surface of the earth. When the sky is overcast, dispersed radiation will not be uniformly distributed.

Short-wave (solar) radiation that has been reflected $I_{r\theta}$. The amount of solar radiation reflected from the ground and reflected onto a surface is determined by the following factors:

$$I_{r\theta} = \left(I_{DN} + d_{d\theta}\right)\rho_g \cdot F_{WG}, \quad (5)$$

where ρ_g, is the reflectivity of the ground or a horizontal surface from where the solar radiation is reflected onto a given surface and F_{WG} ground to the surface. The value of reflectivity is, without a doubt, dependent on the surface characteristics of the ground.

The following equation gives the value of the angle factor F_{WG} in terms of the tilt angle:

$$F_{WG} = \left(1 + \cos\varepsilon\right)/2\,. \quad (6)$$

As a result, for horizontal surfaces (ε=0°), the factor F_{WG} is equal to 0, but for vertical surfaces (ε=90°), the factor F_{WG} is equal to 0.5 [18–20].

5. Results of a dual-axis solar tracker system

5. 1. Temperature comparison of the solar cell

The temperature of both the fixed and tracker solar cell was measured using a thermometer throughout the day on 10 and 11 September as shown in Fig. 11, 12. The experiments were conducted on the two hottest days in Libya to test the device in the hottest environmental conditions. If the device works in the severest conditions, it will certainly work in the least severe conditions.

The graphs in Fig. 11, 12 show that the mobile cell has a high temperature compared to the stationary and this is due for its direct exposure to the sun's rays, let's also notice a slight decrease on September10 at 11:11 due to the sky being partially overcast.

5. 2. Comparison of the intensity of solar radiation falling on the solar cell

Measuring the intensity of solar radiation falling on the fixed solar cell and tracker throughout the day, let's note through the graph shown in Fig. 13, 14, which represents the change in the intensity of solar radiation of the fixed cell and tracker during the daytime hours on days 10 and 11.

Where notice the difference in the change in the values of the radiation intensity of the tracker and the fixed cell. For the traced cell, its radiation intensity is higher than that of the fixed cell and reaches a maximum value of 1282 W/m^2 for September 10 and 1028W/m^2 for September 11, during 11:13 and then begin to decline with sunset.

5. 3. Short circuit current (Isc)

Through the graph shown in Fig. 15, 16, which represents the change in the intensity of the current, where let's notice the difference in the shorting of the fixed cell and the tracker during the daylight hours of the 10th and 11th days. The current values of the tracer and stationary cell change.

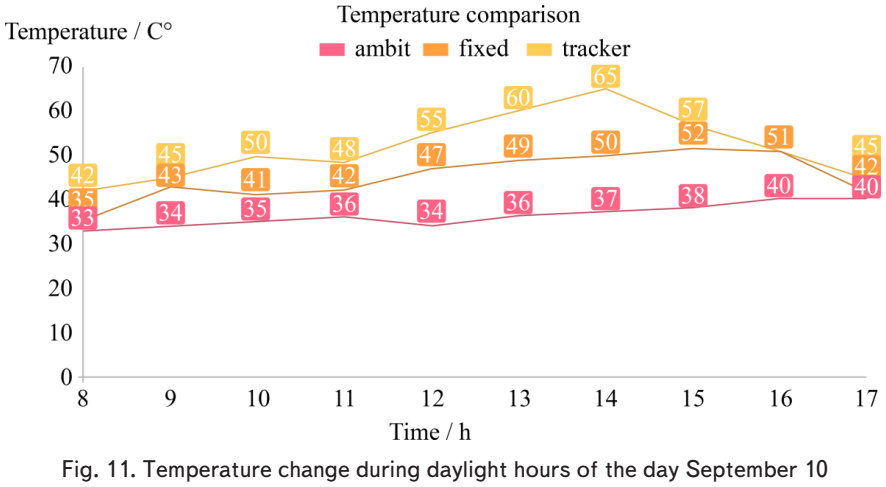

Fig. 11. Temperature change during daylight hours of the day September 10

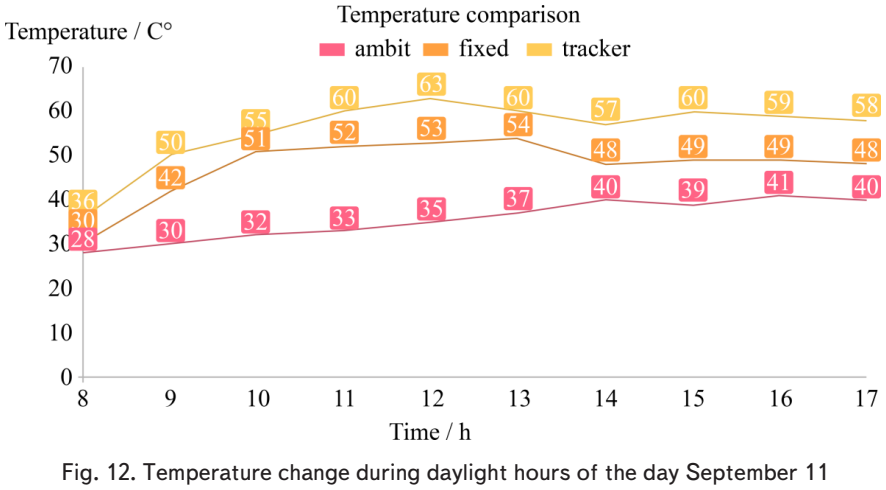

Fig. 12. Temperature change during daylight hours of the day September 11

For the tracker cell, the intensity of it short-circuit current is higher than that of the fixed cell and reaches a maximum value of 4.30 A for the day of September 10 and 3.60 A For the day of September 11, during 11:12, then it begins to decrease according to the solar radiation, while the values of the short-circuit current decrease for the fixed cell compared to the tracking cell.

5. 4. Open circuit voltage (Voc)

In Fig. 17, 18, it is seen that there is a slight change in the value of voltage with time for the fixed and tracker cells during daylight hours.

Its value is slightly lower for the tracker compared to the fixed, and this is due to the high temperature of the latter relative to the fixed.

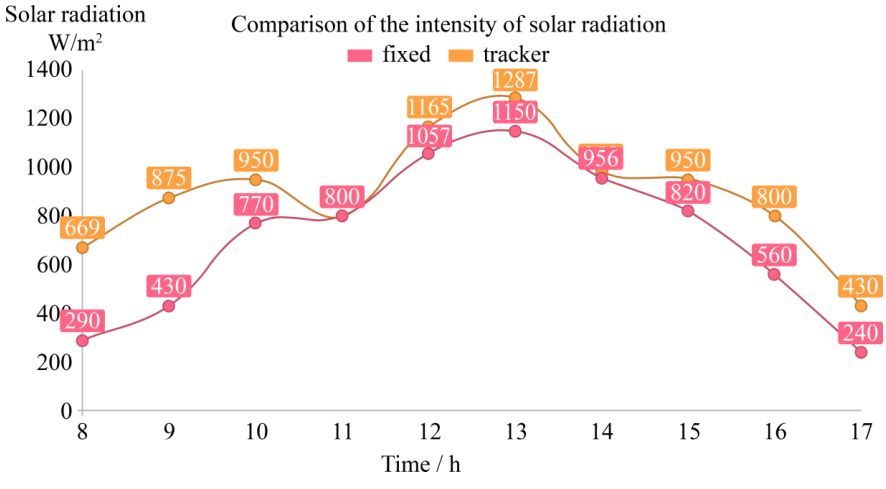

Fig. 13. Intensity of solar radiation for a day September 10

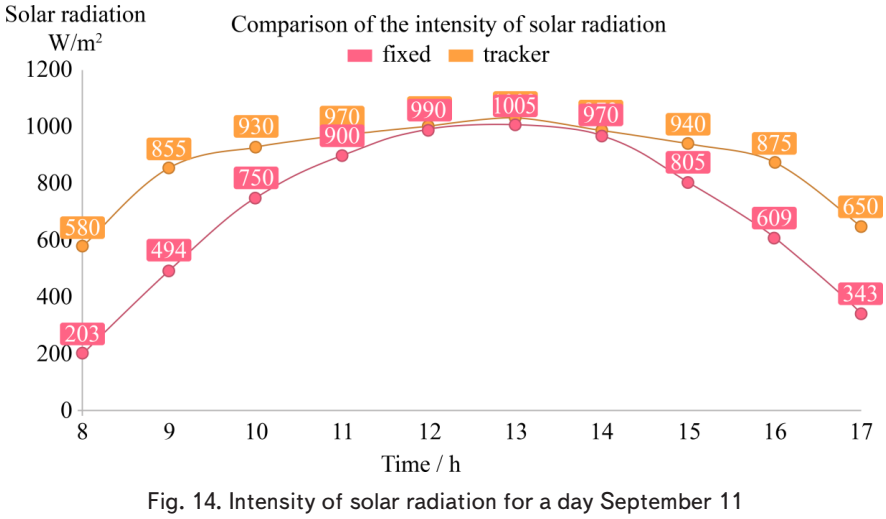

Fig. 14. Intensity of solar radiation for a day September 11

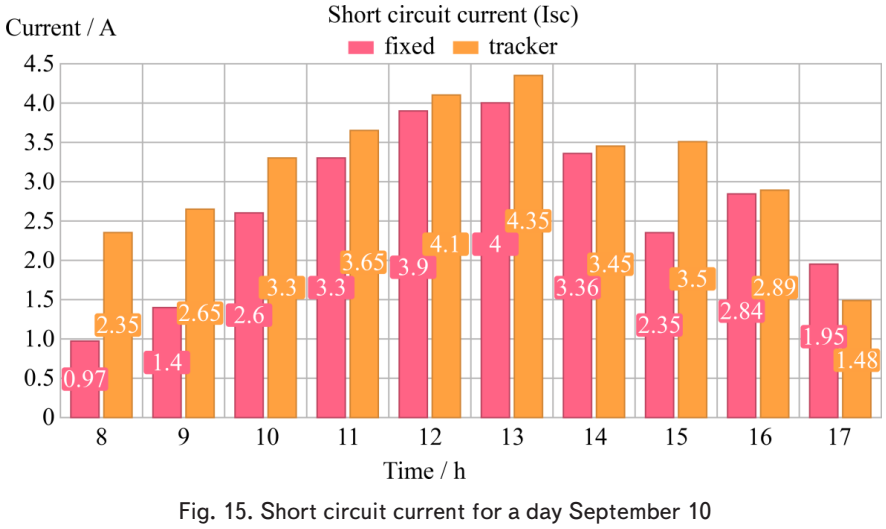

Fig. 15. Short circuit current for a day September 10

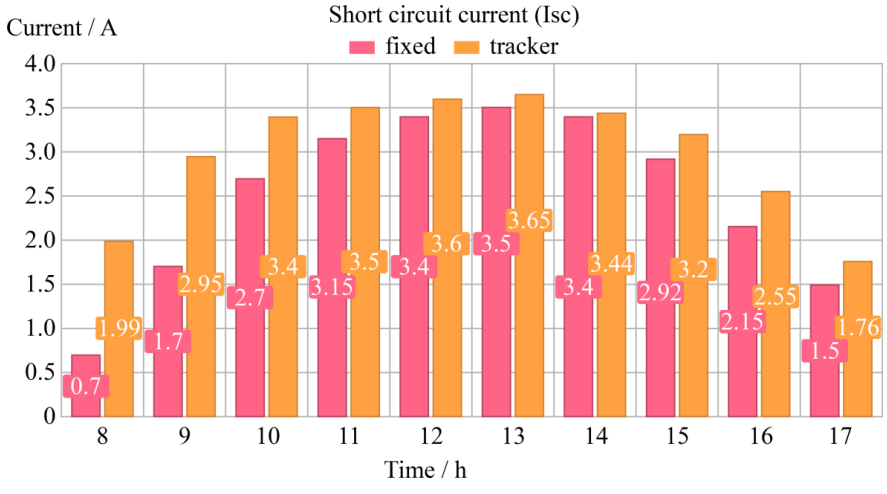

Fig. 16. Short circuit current for a day September 10

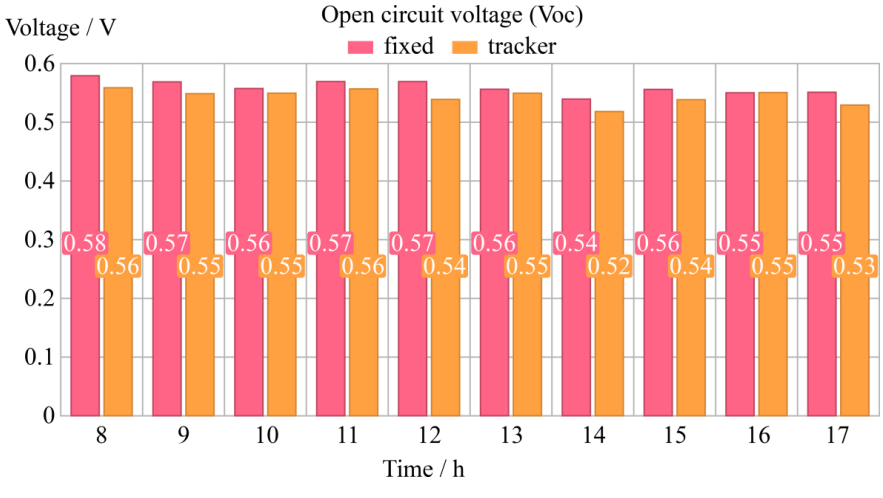

Fig. 17. Voltage changes for a day September 10

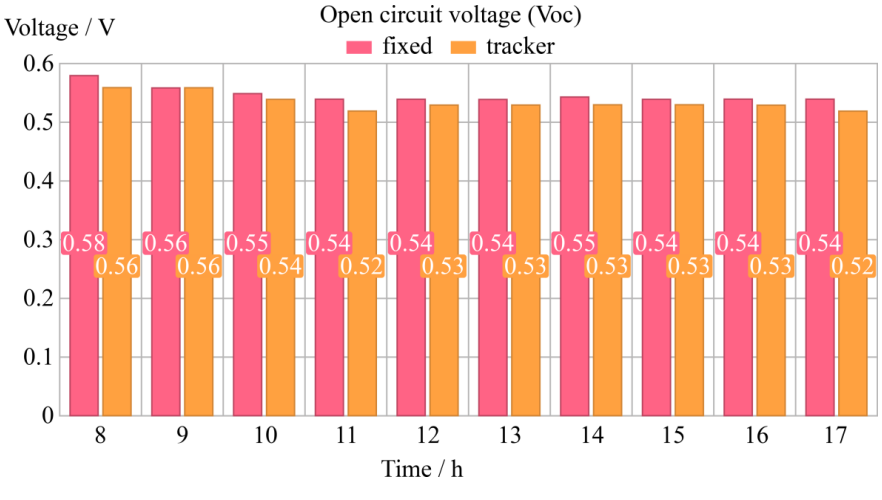

Fig. 18. Voltage changes for a day September 11

5. 5. Power output versus time as a tracker and fixed

Compared to each other, the power outputs of the tracker and fixed states are extremely near in Fig. 19. When comparing the Tracking and No Tracking statuses from morning to noon, the Tracking status produces a greater output. There is virtually little difference in the findings from noon to sunset. When comparing the tracer cell to the stationary cell, the average power obtained from the tracer cell is around 12 % greater.

It is believed that the decreased energy gain from the tracker is due to a greater temperature in the cell as a result of increased solar radiation and a higher ambient temperature, which results in a reduced efficiency of the tracker.

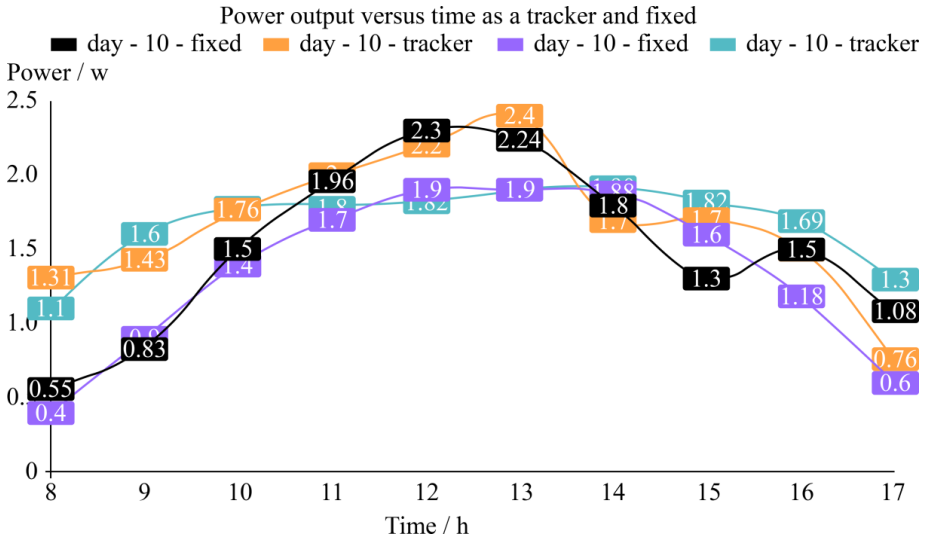

Fig. 19. Power output versus time as a tracker and fixed

6. Discussion of a dual-axis solar tracker system

On September 10 and 11, as shown in Fig. 11, 12, a thermometer was used to record the temperature of both the fixed and tracker solar cells during the course of the day. That the mobile cell has a higher temperature than the stationary one and that this is because of its close proximity to the sun. Observe a little decline on September 10 at 11:11 as a result of the partly cloudy sky.

On September 10 and 11, as shown in Fig. 13, 14, during the afternoon, we took measurements of the amount of solar radiation hitting the stationary solar cell and tracker. The radiation intensity for the traced cell is greater than that of the fixed cell and reaches a maximum value of 1282 W/m^2 on September 10 at 11:13. It subsequently starts to decrease with the setting sun.

During the daylight hours of the 10th and 11th days, compare the shorting of the fixed cell and the tracker, as shown in Fig. 15, 16. The tracker cells short-circuit current peaks at 4.30 A on September 10 and 3.60 A on September 11, respectively, before starting to decline in response to solar light.

Due to the fixed cell's higher temperature, the voltage with time is somewhat lower for the tracker cell during the day than it is for the fixed cell, as shown in Fig. 17, 18. The degree of tension between the two varies somewhat during the day, as can be seen in the image below.

From dawn to noon, the Tracking state generates a higher output as compared to the No Tracking condition, as shown in Fig. 19. The results are almost same from midday till dusk. It is thought that the increased temperature in the cell brought on by more solar radiation and a warmer environment is the cause of the tracker's lower energy gain.

The LDR tracking system required large and expensive parts for integrated development, as this was the biggest limitation for us.

The objectivity of manufacturing that gives 100 % inaccurate results due to the small size of the tracking system.

In the future it is possible to make a large tracking system that can capture the sun's rays, and it is better and more efficient.

7. Conclusions

1. The temperature of both the fixed and tracker solar cell was measured using a thermometer throughout the day on September 10 and 11. That the mobile cell has a high temperature compared to the stationary and this is due for its direct exposure to the sun's rays. Also, noticed a slight decrease on September 10 at 11:11 due to the sky being partially overcast.

2. During the daytime hours of September 10 and 11, we measure the intensity of solar radiation falling on the fixed solar cell and tracker. For the traced cell, its radiation intensity is higher than that of the fixed cell and reaches a maximum value of 1282 W/m^2 for September 10 – during 11:13 – and then begin to decline with sunset.

3. Measure the difference in the shorting of the fixed cell and the tracker during the daylight hours of the 10th and 11th days. The tracker cell's short-circuit current reaches a maximum value of 4.30 A for the day of September 10 and 3.60 A for September 11, then it begins to decrease according to the solar radiation.

4. The tension in the vacuum for the fixed and tracker cells during daylight hours is slightly lower for the tracker compared to the fixed, and this is due to the high temperature of the latter. It is seen that there is a slight change in the value of tension between the two at different times of the day.

5. When comparing of power output between the Tracking and No Tracking statuses from morning to noon, the Tracking status produces a greater output (2.4 and 2.24 W respectively). There is virtually little difference in the findings from noon to sunset. It is believed that the decreased energy gain from the tracker is due to a greater temperature in the cell as a result of increased solar radiation and a higher ambient temperature.

Conflict of interest

The authors declare that they have no conflict of interest in relation to this research, whether financial, personal, authorship or otherwise, that could affect the research and its results presented in this paper.

References

1. Atallah, F. S., Mahmood, Yaseen. H. H., Tawfeeq, S. S. . (2018). Fabrication and study of solar panel tracking system. Tikrit Journal of Pure Science, 23 (1), 123–127. doi: https://doi.org/10.25130/tjps.23.2018.017
2. Jamroen, C., Komkum, P., Kohsri, S., Himananto, W., Panupintu, S., Unkat, S. (2020). A low-cost dual-axis solar tracking system based on digital logic design: Design and implementation. Sustainable Energy Technologies and Assessments, 37, 100618. doi: https://doi.org/10.1016/j.seta.2019.100618
3. Fernández-Ahumada, L. M., Ramírez-Faz, J., López-Luque, R., Varo-Martínez, M., Moreno-García, I. M., Casares de la Torre, F. (2020). A novel backtracking approach for two-axis solar PV tracking plants. Renewable Energy, 145, 1214–1221. doi: https://doi.org/10.1016/j.renene.2019.06.062
4. Dold, R. H. (2007). Literature review, no. 0215199, 11.
5. Rizk, J. C. A. Y., Chaiko, Y. (2008). Solar tracking system: more efficient use of solar panels. World Academy of Science, Engineering and Technology, 41, 313–315.
6. Barsoum, N., Vasant, P. (2010). Simplified solar tracking prototype. Global Journal of Technology and Optimization GJTO, 1, 38–45.
7. Kancevica, L., Putans, H., Ziemelis, I. (2012). The tracking system for solar collectors with reflectors. In Proceeding of the International Scientific Conference on Renewable Energy and Energy Efficiency. Jelgava, 190–195.
8. Racharla, S., Rajan, K. (2017). Solar tracking system – a review. International journal of sustainable engineering, 10 (2), 72–81.
9. Rubio, F. R., Ortega, M. G., Gordillo, F., López-Martínez, M. (2007). Application of new control strategy for sun tracking. Energy Conversion and Management, 48 (7), 2174–2184. doi: https://doi.org/10.1016/j.enconman.2006.12.020
10. Amadi, H. N., Gutierrez, S. (2019). Design and Performance Evaluation of a Dual-Axis Solar Tracking System for Rural Applications. European Journal of Electrical Engineering and Computer Science, 3 (1). doi: https://doi.org/10.24018/ejece.2019.3.1.52
11. Nguyen, B. T., Ho, H.-X. T. (2020). Design, Implementation and Performance Analysis of a Dual Axis Solar Tracking System. Advances in Science, Technology and Engineering Systems Journal, 5 (3), 41–45. doi: https://doi.org/10.25046/aj050306
12. Sumathi, V., Jayapragash, R., Bakshi, A., Kumar Akella, P. (2017). Solar tracking methods to maximize PV system output – A review of the methods adopted in recent decade. Renewable and Sustainable Energy Reviews, 74, 130–138. doi: https://doi.org/10.1016/j.rser.2017.02.013
13. Peter, J. N., Kanyarusoke, K. E. (2019, March). Design optimization of pillar-mounted sun tracking solar-water purifiers for large households. 2019 International Conference on the Domestic Use of Energy (DUE), IEEE, 169–175.
14. Tsoy, A., Titlov, O., Granovskiy, A., Koretskiy, D., Vorobyova, O., Tsoy, D., Jamasheva, R. (2022). Improvement of refrigerating machine energy efficiency through radiative removal of condensation heat. Eastern-European Journal of Enterprise Technologies, 1 (8 (115)), 35–45. doi: https://doi.org/10.15587/1729-4061.2022.251834
15. Elmnifi, M., Moria, H., Elbreki, A. M., Abdulrazig, O. D. (2021). Possibilities Study of Using Hybrid Solar Collectors in Northeastern Libya Residential Home. International Journal of Renewable Energy Research, 11 (2), 654–661. doi: https://doi.org/10.20508/ijrer.v11i2.11938.g8186
16. Safaripour, M. H., Mehrabian, M. A. (2011). Predicting the direct, diffuse, and global solar radiation on a horizontal surface and comparing with real data. Heat and Mass Transfer, 47 (12), 1537–1551. doi: https://doi.org/10.1007/s00231-011-0814-8
17. Jamil, B., Akhtar, N. (2017). Comparison of empirical models to estimate monthly mean diffuse solar radiation from measured data: Case study for humid-subtropical climatic region of India. Renewable and Sustainable Energy Reviews, 77, 1326–1342. doi: https://doi.org/10.1016/j.rser.2017.02.057
18. Bakirci, K. (2012). The Calculation of Diffuse Radiation on a Horizontal Surface for Solar Energy Applications. Energy Sources, Part A: Recovery, Utilization, and Environmental Effects, 34 (10), 887–898. doi: https://doi.org/10.1080/15567031003699525
19. Nakashydze, L. V., Hilorme, T. V. (2015). Energy security assessment when introducing renewable energy technologies. Eastern-European Journal of Enterprise Technologies, 4 (8 (76)), 54–59. doi: https://doi.org/10.15587/1729-4061.2015.46577
20. Kobeyeva, Z., Khussanov, A., Atamanyuk, V., Hnativ, Z., Kaldybayeva, B., Janabayev, D., Gnylianska, L. (2022). Analyzing the kinetics in the filtration drying of crushed cotton stalks. Eastern-European Journal of Enterprise Technologies, 1 (8 (115)), 55–66. doi: https://doi.org/10.15587/1729-4061.2022.252352